ADVANCED MATERIALS

Wafer Bonding and Layer Splitting for Microsystems**

By Qin-Yi Tong* and Ulrich M. Gösele

In advanced microsystems various types of devices (metal-oxide semiconductor field-effect transistors, bipolar transistors, sensors, actuators, microelectromechanical systems, lasers) may be on the same chip, some of which are 3D structures in nature. Therefore, not only materials combinations (integrated materials) are required for optimal device performance of each type but also process technologies for 3D device fabrication are essential. Wafer bonding and layer transfer are two of the fundamental technologies for the fabrication of advanced microsystems. In this review, the generic nature of both wafer bonding and hydrogen-implantation-induced layer splitting are discussed. The basic processes underlying wafer bonding and the layer splitting process are presented. Examples of bonding and layer splitting of bare or processed semiconductor and oxide wafers are described.

1. Introduction

"Wafer bonding" refers to the phenomenon that mirror-polished, flat, and clean wafers, when brought into contact at room temperature, bond to each other without using adhesives or external forces. The phenomenon that optically polished pieces can adhere or bond to each other has been known for a long time and was first studied by Rayleigh in 1936[1] for quartz glass. But it was only in 1985 that an attempt was made almost simultaneously by researchers at Toshiba[2] and IBM[3] to use this room-temperature adhesion phenomenon coupled with an appropriate heating step for silicon wafers in order to replace epitaxial growth of thick silicon wafers or to fabricate silicon-on-insulator (SOI) structures, respectively. Shortly afterwards, as an extension of the well-established "anodic bonding", the bonding of structured silicon wafers was applied to the fabrication of micromachined pressure sensors, termed "silicon fusion bonding".[4] It has been demonstrated that wafer bonding is not restricted to silicon/silicon bonding but can be applied to many kinds of materials combinations involving silicon or other materials.[5] The generic nature of wafer bonding was recognized in the early nineties[6] and it is one of the two main topics of this review and will be discussed in more detail based on recent developments.

In many wafer bonding applications, thinning of one wafer of a bonded pair is a necessary step to realize the desired materials combination. In SOI, a thin single crystalline silicon layer is employed to make devices. Its thickness is in the range of 5 nm to a few micrometers, depending on the device structures. In the case of bonding of dissimilar materials, thinning of one wafer of a pair to a thickness less than the respective critical value for the materials combination is essential. This approach prevents the generation of misfit dislocations in the layer and avoids cracking of the bonded pairs during subsequent thermal processing steps.[7] The most promising approach to realizing layer transfer involves using wafer bonding and hydrogen-implantation-induced layer splitting from the host wafer to a bonded desired substrate.[8] This approach has been applied to Si (SOI), Ge,[9] SiC,[10,11] InP,[12] and GaAs[13] layer transfer; among these, SOI wafers are now in mass production. Fully processed or partially processed device layers can also be transferred from the host materials onto a desired substrate and the back side of the device layer can then be further processed for an improved device performance. The 3D double-gate SOI MOSFET (metal oxide semiconductor field effect transistor) has been considered as a promising candidate for ultra-small devices with a gate length of about 25 nm for future VLSI (very large scale integration) circuits. Several designs of the device have been reported, and wafer bonding and layer transfer appear to be essential.[14] Recently, layer transfer of oxides such as sapphire and $LaAlO_3$ has also been demonstrated.[15] The generic nature of H-implantation-induced layer splitting is just beginning to be recognized[16] and it is therefore one of the subjects of this review.

In the following, we will first discuss our present understanding of the wafer bonding process. The general re-

[*] Prof. Q.-Y. Tong
Research Triangle Institute
RTP, NC 27709 (USA)
Prof. U. Gösele
Max Planck Institute of Microstructure Physics
Weinberg 2, D-06120 Halle (Germany)
Prof. Q.-Y. Tong, Prof. U. Gösele
School of Engineering, Duke University
Durham, NC 27708 (USA)

[**] We thank the members of the wafer bonding research groups at Duke University and at the Max Planck Institute of Microstructure Physics in Halle, Germany for their contributions to the wafer bonding research reported in this paper. The support of the Center of Semiconductor Research at Research Triangle Institute is greatly appreciated. We are grateful for the technical assistance in CMP by Tao Zhang, R. Rhoades, and A. Clark of Rodel, Inc. Part of the research was supported by grants of SEH, Japan and Intel (Duke University) and by the German Federal Ministry of Science, Education, Research and Technology under contracts BMBF-13N6758/0 and BMBF-13N6451/1.

 © WILEY-VCH Verlag GmbH, D-69469 Weinheim, 1999 0935-9648/99/1712-1409 $ 17.50+.50/0

quirements of wafer conditioning for successful wafer bonding are described in terms of the process building blocks of wafer bonding: surface preparation, room-temperature bonding, low-temperature bond enhancement, and maintaining a bubble-free bonding interface (Sec. 2). Then we turn to the essential mechanisms involved in the H-implantation-induced layer splitting process. The conditions under which layer splitting can be achieved are discussed in terms of layer splitting modules: platelet generation, hydrogen molecule formation in microcracks, and layer cleavage (Sec. 3). Finally, examples of wafer bonding and layer splitting applications are presented (Sec. 4). In this review we will not try to be exhaustive in terms of references but refer to recent conference proceedings,[17–20] review articles,[21–25] a special 1995 issue of the *Philips Journal of Research*,[26] and a book on this subject.[27]

2. Process Modules of Wafer Bonding

The basic requirements for good wafer bonding are: i) the materials being bonded form a covalent or chemical bond across their interface, ii) high stresses are avoided, and iii) no interface bubbles develop. The basic process modules to achieve these goals of wafer bonding are i) surface preparation, ii) room-temperature bonding, iii) low-temperature bond enhancement, and vi) maintaining a bubble-free bonding interface.

2.1. Surface Preparation

2.1.1. Surface Smoothness

The phenomenon of wafer direct bonding originates from the intermolecular forces of attraction between two contacting surfaces. Therefore, the first step in the wafer bonding process is appropriate wafer surface preparation for bonding (contacting) at room temperature using no adhesive or external forces. Physically, the bonding surfaces should be sufficiently smooth and flat. Chemically, the surfaces must be sufficiently clean and preferably terminated by a couple of monolayers of bonding species.

It is well known that electrically polarized (identical or different) molecules are attracted to each other by so-called van der Waals intermolecular interactions. There are three types of van der Waals forces:[6] the dipole–dipole force between two polar molecules, the dipole-induced force between a polar and a non-polar molecule, and the dispersion force between two non-polar molecules resulting from the non-zero average value of the square of the temporary dipole moment due to charge distribution fluctuations.[28] Therefore, van der Waals forces ubiquitously exist between almost all substances. The force acting between two macroscopic bodies is the result of many-body effects. The pairwise summation of all of the interatomic forces acting between all of the atoms of the two bodies plus any additional medium can be considered as a first approximation of the force acting between the two bodies.

Qin-Yi Tong is Adjunct Professor at the School of Engineering at Duke University and manager of the Wafer Bonding Laboratory at the Research Triangle Institute. He was a consultant at the Max Planck Institute of Microstructure Physics in Halle, Germany from 1995 to 1998. He has been Director and Professor of the Microelectronics Center at Southeast University in Nanjing, China since 1985, where he began wafer bonding research. He came to Duke University in 1991 and has been carrying out research and teaching in the field of wafer bonding there ever since. Prof. Tong has published 169 papers, 4 books, and 15 patents or disclosures since 1982. Together with Dr. U. Gösele he wrote the first book on wafer bonding, which was published by Wiley in 1998.

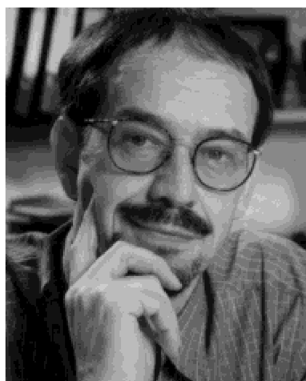

Ulrich M. Gösele has been a director at the Max Planck Institute of Microstructure Physics, Halle, Germany since 1993. For many years he was a J.B. Duke Professor of Materials Science at Duke University in North Carolina. Prior to that he worked at the Siemens Research Laboratories in Munich. He has had visiting appointments at IBM's Watson Research Center, the NTT LSI Laboratories in Atsugi, Japan, and the Atomic Energy Board in South Africa. His research interests include defects and diffusion process in semiconductors, quantum effects in porous silicon, self-organized structure formation, and semiconductor wafer bonding. He holds numerous patents on wafer bonding technology and has co-organized various symposia in this field. Together with Prof. Q.-Y. Tong he wrote the first book on semiconductor wafer bonding.

© WILEY-VCH Verlag GmbH, D-69469 Weinheim, 1999
0935-9648/99/1712-1410 $ 17.50+.50/0

The surface force F between two bodies decreases rapidly with distance t, e.g., with the inverse third power for flat plates (Eq. 1).

$$F \sim t^{-3} \quad (1)$$

Based on the above discussion, it is clear that two solid-state plates of almost any materials can be bonded to each other at room temperature provided that their surfaces are sufficiently smooth to allow the surface molecules of two plates to get close enough and the van der Waals forces between atoms on the touching surfaces to be sufficiently strong. The smoothness of wafer surfaces required for successful bonding mainly depends on the type and strength of the forces of interaction at the bonding interface. Bonding by the dispersion force, which is weak and exists between any substances, requires extremely smooth surfaces, which may only be achieved by expensive optical polishing.

There is an especially strong form of dipole–dipole attraction termed hydrogen bonding in which the hydrogen atom in a polar molecule interacts with an electronegative atom of either an adjacent molecule or the same molecule. A hydrogen atom can participate in a hydrogen bond if it is bonded to oxygen, nitrogen, or fluorine because H–F, H–O, and H–N bonds are strongly polarized, leaving the hydrogen atom with a partial positive charge. This electrophilic hydrogen has a strong affinity for non-bonding electrons so that it can form intermolecular attachments with an electronegative atom such as oxygen, nitrogen, or fluorine. For instance, water is a polarized molecule consisting of hydrogen as well as oxygen, which allows hydrogen bonds to form between water molecules themselves. If two mating surfaces are terminated by water molecules, the H···O hydrogen bonding between water molecules across the mating surfaces results in a strong van der Waals force of attraction. The hydrogen bond energy of ~0.20 eV is about 10 % of a normal Si–Si covalent bond energy of 1.9 eV. Since a cluster of two or three water molecules is energetically more favorable than an isolated water molecule,[29] the linkage of water molecules may form a bridge between the two mating surfaces. In this way a "long-range" intermolecular force can be realized[30] and the requirement of surface smoothness for room-temperature bonding is greatly eased. Similarly, HF and NH_3 molecules are expected to have the same function as water molecules in wafer bonding, as evidenced by the bonding of HF-dipped hydrophobic Si wafers,[31] HF bonding of SiO_2/SiO_2,[32] and NH_4OH-treated SiO_2-covered wafer bonding.[2,33]

It is known that a bare Si surface is usually covered by a native oxide layer. Si wafers can also be oxidized thermally. Chemicals with OH^-, H^+, or F^- can attack Si–O–Si bonds and form Si–OH or Si–F groups on the surfaces of bare or oxidized Si wafers. The polar OH groups can form hydrogen bonds readily with water molecules. Figure 1 shows schematically the bridge of water molecules between two SiO_2 surfaces. Since the size of an OH group is 1.01 Å and the distance between two hydrogen-bonded oxygen atoms in ice is 2.76 Å, a bridge of three hydrogen-bonded water molecules has a length of about 10 Å. It implies that two SiO_2 surfaces that are separated by up to 10 Å (average surface roughness of 5 Å) can adhere to each other by hydrogen bonding at room temperature.[33] This implication is supported by results of infrared (IR) spectroscopy measurements[42] and other experimental observations.[34] Since commercially available Si wafers have a mean surface roughness of about 1 Å they can bond to each other readily at room temperature. Similarly, chemicals containing OH^-, H^+, or F^- ions can also attack the Si–N–Si bond to form Si–OH, Si–F, or Si–NH groups[35] for hydrogen bonding.

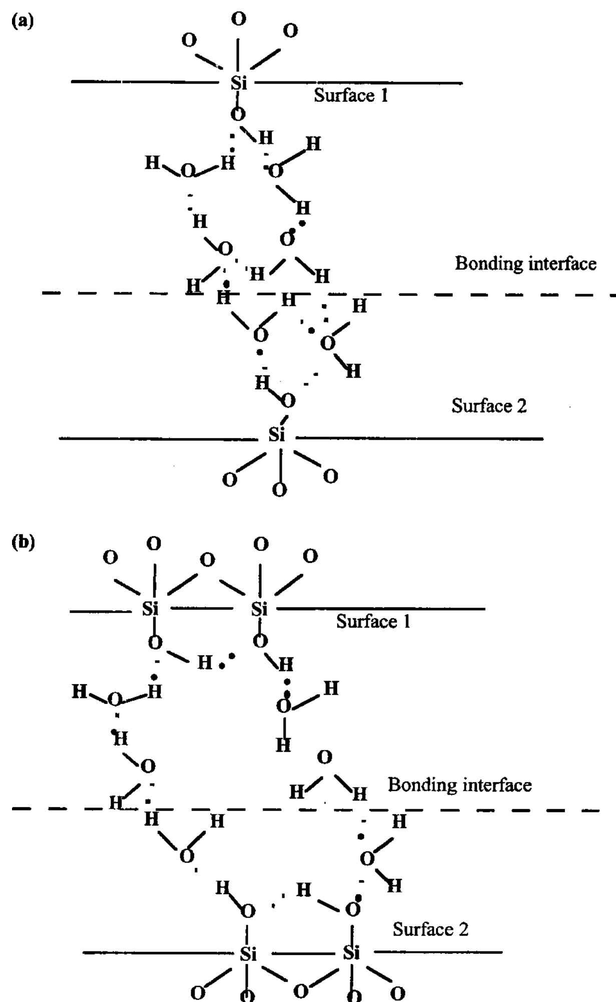

Fig. 1. Schematics of water bridging between two hydrophilic Si bonding wafers on a) isolated and b) associated Si–OH groups.

The smoothness discussed above is a *microscopic* property of bonding surfaces that determines the strength of the forces of attraction or the bonding energy. It should be noted that conventionally bonding energy between two mating surfaces is the sum of the surface energies of the two surfaces at the time immediately after they are separated. If the bonding wafers are identical the total bonding energy is two

 © WILEY-VCH Verlag GmbH, D-69469 Weinheim, 1999 0935-9648/99/1712-1411 $ 17.50+.50/0

times that of the specific surface energy of one of the bonded wafers. For convenience, in this paper the bonding energy is defined as the average specific surface energy of the two bonding surfaces when the bonded pair is partially separated by a separator such as a razor blade of thickness t_b,[36] as schematically shown in Figure 2. If the bonded wafers are identical the bonding energy refers to the specific surface

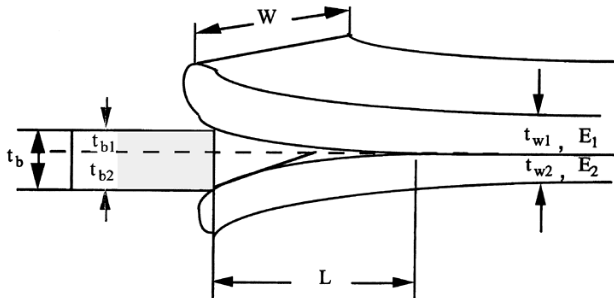

Fig. 2. Schematic of the crack-opening method for surface energy measurement.

energy of one of the bonded wafers. The bonding energy or surface energy can be estimated from the bond density at the interface and the bond energy of each bond.[27] Experimentally, the bonding energy can be determined by measuring the equilibrium crack length when a separator is inserted into the bonding interface.[36] This method is based on the equilibrium between the elastic forces of the bent separated part of a pair and bonding forces at the crack tip. In the case of bonded pairs with identical wafers of thickness t_w and $E_1 = E_2 = E$ where E is Young's modulus, the bonding energy γ can be obtained from the equilibrium crack length L:[36]

$$\gamma = \frac{3\,E t_w^3 t_b^2}{32\,L^4} \qquad (2)$$

For wafers of different thickness and/or elastic properties analogous formulae are available.[27] The bonding energy γ is typically around 100 mJ/m^2 for room-temperature-bonded hydrophilic Si surfaces and around 20 mJ/m^2 for (hydrogen-covered) hydrophobic Si surfaces prepared by an HF dip.[31] It is clear that there are usually many microgaps at the bonding interface of room-temperature-bonded wafer pairs, resulting from the microroughness of the bonding surfaces as shown in Figure 3. In order to reach a full bonding strength the microgaps will have to be closed. As

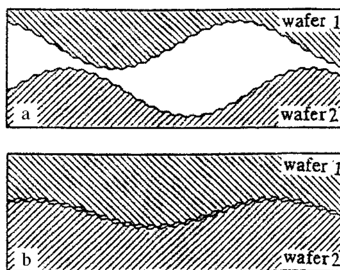

Fig. 3. Schematic of a) wafer surfaces before bonding and b) bonding interface of room-temperature-bonded pairs.

we will discuss later, this can be realized by increased bonding energy and/or oxidation or atom migration during subsequent annealing at elevated temperatures.

2.1.2. Surface Flatness

Bonding surfaces of two wafers are never perfectly flat. Local unbonded regions can result from the gaps at the bonding interface caused by the waviness of the mating surfaces. The flatness, non-uniformity, or waviness is a global and macroscopic property of bonding surfaces. Wafers with sufficiently smooth surfaces but having a certain degree of waviness may still bond to each other because the elastic deformation of the two bonding wafers can accommodate this scale of surface waviness, as schematically shown in Figure 3. The resultant stress at the bonding interface is in the 1×10^7 N/m^2 range, which is much less than that required to nucleate dislocations and to plastically deform Si (2.5×10^9 N/m^2), and should not affect the structural properties of Si wafers of the bonded pairs.[37]

Whether two wafers bond or not depends not only on the bonding energy at room temperature but also on the height $2h$ and the extension $2R$ of the gaps at the bonding interface, see Figure 4. For $R > 2t_w$ (Fig. 4a) the condition for gap closing is given by

$$h < \frac{R^2}{\sqrt{\frac{2}{3}\frac{E'\,t_w^3}{\gamma}}} \qquad (3)$$

where E' is given by $E/(1-\nu^2)$ with ν being Poisson's ratio. For $R < 2t_w$ (Fig. 4b) the condition for gap closing is independent of the wafer thickness t_w and is given by

$$h < 3.6\,(R\gamma/E')^{1/2} \qquad (4)$$

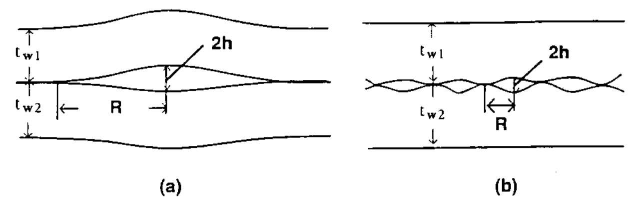

Fig. 4. Schematic of gaps between wafers for the case of a) $R > 2t_w$ and b) $R < 2t_w$.

In Figure 5 the regions of gap closing or not closing are shown for two Si wafers of equal thickness t_w based on γ = 100 mJ/m^2 for various values of t_w. For structured wafers, in Equations 3 and 4 γ may be replaced approximately by $f_b\gamma$ where f_b is the ratio between the interface area in contact and the whole wafer area.[38] In practice, the flatness variation of 1–3 µm over commercial 4 inch (1 inch = 2.54 cm) Si wafers poses no obstacle to wafer bonding at room temperature. Bow and warpage of wafers up to about 25 µm are also tolerable. In reality the waviness is represented in a whole Fourier spectrum of amplitudes for certain wavelengths. If more than one single spatial frequency (e.g., the

 © WILEY-VCH Verlag GmbH, D-69469 Weinheim, 1999 0935-9648/99/1712-1412 $ 17.50+.50/0

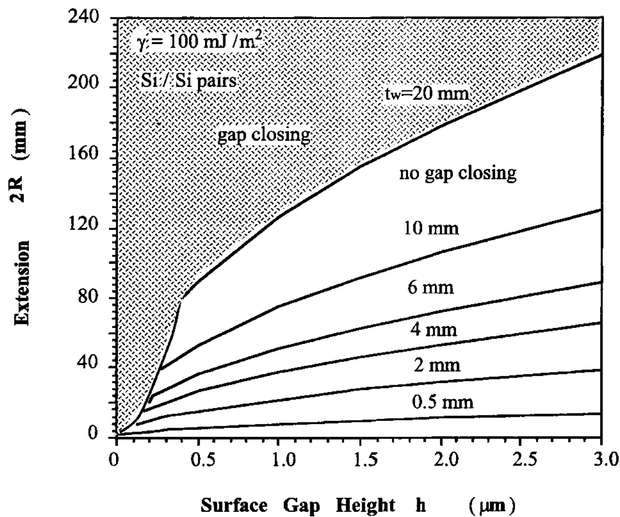

Fig. 5. Parameter combinations of gap height h and lateral extension R of gaps that can be closed for various Si wafer thicknesses and γ = 100 mJ/m^2.

macroscopic bow) is dominating, an integral formulation has to be used. The developed theoretical expressions also show that even infinitely thick pieces can be bonded provided the surface flatness is sufficiently good, as has been known for almost one hundred years to occur with optically polished bulk pieces of glasses or metals. Experimentally, optically polished Si crystals 4 inches in diameter and 20 mm thick with a surface flatness variation of 630 Å have been bonded successfully at room temperature.[39]

In summary, it appears that a wafer of any material can be bonded at room temperature to another wafer of the same or a different material via van der Waals intermolecular forces provided that the bonding surfaces are sufficiently smooth, flat, and preferably terminated by a couple of monolayers of bonding species.

2.2. Room-Temperature Bonding

After surfaces of bonding wafers are properly prepared to be sufficiently smooth and flat, the two wafers can readily bond to each other at room temperature when they are brought into contact in air, as shown in Figure 3. However, interface bubbles may form at this stage for one of the following reasons: 1) particulate contamination on the surfaces, 2) trapped air at the bonding interface.

A particle with a diameter of $2h$ can form an unbonded interface area or bubble with a diameter of $2R$ for $R > 2t_w$:

$$R = (0.67\, E' t_w^3/\gamma)^{1/4}\, h^{1/2} \tag{5}$$

A particle of about 1 μm diameter leads to an unbonded area with a diameter of about 0.5 cm for typical 4 inch diameter Si wafers with a thickness of 525 μm.

In order to avoid getting particles between the wafers during room-temperature bonding, after wafer cleaning procedures wafers are bonded in air either in a conventional cleanroom of class 10 or better or in a so-called microcleanroom. Using a microcleanroom,[40] two wafers are placed face to face and separated by spacers to about a couple of millimeters and deionized water is flushed through the gap between the two wafers to remove particles that are weakly attached to the wafer surfaces during the room-temperature bonding operation (see Fig. 6).

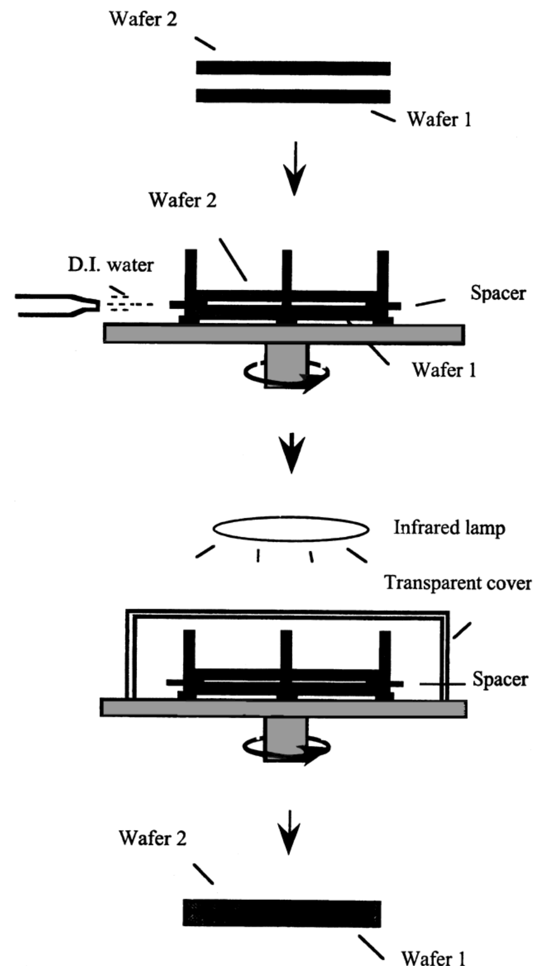

Fig. 6. Schematic of microcleanroom set-up and procedure.

Trapped air bubbles at the bonding interface are usually caused by the spreading of bonding areas starting from more than one location at the bonding interface. To prevent trapped air bubbles, when two wafers are brought into contact bonding is usually initiated at only one point by slightly pressing the wafers together locally. The bonded area then spreads over the whole wafer in a couple of seconds.

2.3. Low-Temperature Bond Enhancement

2.3.1. Polymerization of Bonded OH-Terminated Surfaces

Wafer bonding provides a high degree of flexibility in materials integration. Although differences of bonding materials in terms of composition, crystal structure, crystal ori-

 © WILEY-VCH Verlag GmbH, D-69469 Weinheim, 1999 0935-9648/99/1712-1413 $ 17.50+.50/0

entation, wafer thickness, doping type, and profile do not present obstacles to wafer bonding, thermal mismatch imposes a severe restriction on the temperatures of the annealing following room-temperature bonding to increase the bonding energy. Therefore, it is crucial to achieve strong bonding by low-temperature annealing. Here "low" means relatively moderate temperatures typically in the range 23–400 °C. Low-temperature bonding is also essential for bonding of processed wafers or compound materials to prevent undesirable changes or decomposition even if the bonding wafers are thermally matched.

As mentioned above, bonding surfaces covered with silicon oxide or nitride can form hydrogen bonds if an activation treatment in chemicals containing OH^-, H^+, or F^- ions to form Si–OH, Si–F, or Si–NH groups is performed prior to room-temperature bonding. For RCA- (RCA1: $H_2O/H_2O_2/NH_4OH$ = 5:1:1; RCA2: $H_2O/H_2O_2/HCl$ = 5:1:1) treated bare or oxide-covered Si wafers, the surfaces are hydrophilic and are terminated mainly by OH groups. It is known that polymerization of silanol groups (Si–OH) to form strong siloxane (Si–O–Si) covalent bonds can take place at temperatures as low as room temperature provided that these groups are in close proximity and hydrogen bonded:

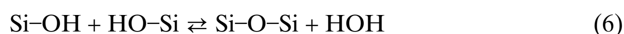

$$\text{Si–OH} + \text{HO–Si} \rightleftarrows \text{Si–O–Si} + \text{HOH} \quad (6)$$

Reaction 6 is reversible at $T < 425$ °C if water is present. For strong siloxane bonds (Si–O–Si) to form across the bonding surfaces excess water has to be removed. It can be done, for instance, via annealing at $T > 110$ °C to remove water molecules that bridge across the bonding wafers. Water can also be generated by the polymerization reaction (Reaction 6). Some water molecules diffuse along the bonding interface to the outside, which is a slow process. Some water molecules may also diffuse through the surrounding native or thermal oxide to react with Si to form SiO_2 and hydrogen:

$$\text{Si} + 2\,\text{HOH} \longrightarrow \text{SiO}_2 + 2\,\text{H}_2 \quad (7)$$

Figure 7 shows the typical bonding energy of hydrophilic Si/Si pairs as a function of annealing temperature.[41] The attainable bonding energy is approximately 50 % of the fracture energy of silicon and ~30 % of the fracture energy of thermal silicon oxide after 150 °C annealing. The integrated IR absorbance of HOH and OH stretching modes obtained from IR spectra of the bonding interface of hydrophilic Si/Si pairs as a function of annealing temperature indicates that 80 % of the molecular water and up to 50 % of the interfacial OH groups have been removed after 70 h of annealing at 150 °C.[42] Hydrogen molecules are small and much easier to diffuse out or dissolve in the oxide than water molecules. Therefore, bonding of a Si wafer with a very thin native oxide layer to a Si wafer covered with a thick oxide layer can readily result in a strong bond at low

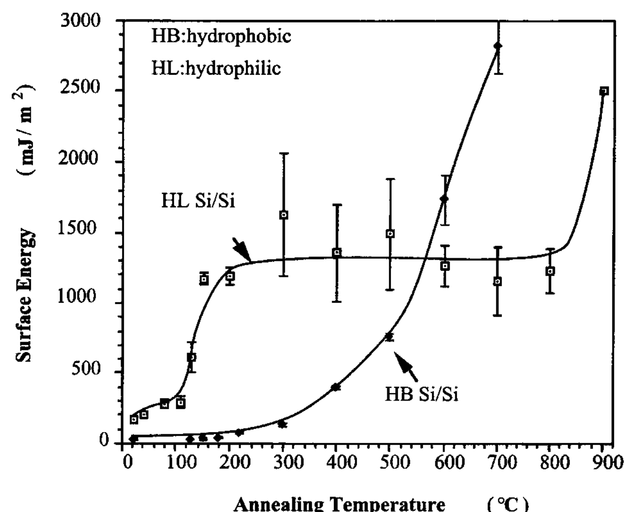

Fig. 7. Bonding energy of bonded hydrophilic and hydrophobic Si wafers measured by the crack opening method as a function of annealing temperature for an annealing time of 100 h at each temperature.

temperature because the thin oxide favors Reaction 7 to remove the water and the thick oxide can absorb the hydrogen to reduce the gas pressure at the bonding interface. The experimental results appear to support this argument.[34] Since the bonding reaction depends only on the bonding surfaces, and a silicon oxide layer can relatively easily be deposited by PECVD (plasma-enhanced chemical vapor deposition) at low temperatures (<200 °C), an oxide layer may be used as the bonding layer for materials other than Si in order to achieve a strong bond at low temperatures.

Bare Si wafers are usually covered by a native oxide layer with a thickness of 2–10 Å. A native oxide is a strained oxide with a much higher chemical reactivity than a thermal oxide. As shown in Figure 7, after standard RCA treatment, the surface of a native oxide is saturated with OH groups (~4.6 OH groups/nm^2) and the bonding energy of bonded bare Si/Si pairs can be equivalent to about half of the bulk Si fracture energy during annealing at a temperature as low as 150 °C and the water produced by Reaction 6 can easily diffuse through the thin oxide layer and be removed as shown in Reaction 7. After 150 °C annealing, the bonding energy of bare Si wafer pairs treated in HNO_3,[43] HCl,[44] or H_2SO_4[44] aqueous solutions before room-temperature bonding is higher than that of RCA-treated pairs. This behavior may be attributed to the increased chemical reactivity of chemically grown oxide on the Si wafer surfaces.

2.3.2. Polymerization of Bonded NH_2-Terminated Surfaces

In order to achieve a strong bond at low temperatures for bonding of Si wafers covered by a relatively thick oxide (SiO_2/SiO_2), it is beneficial to treat the surfaces prior to room-temperature bonding so that they are terminated by species that produce less or no water during

 © WILEY-VCH Verlag GmbH, D-69469 Weinheim, 1999 0935-9648/99/1712-1414 $ 17.50+.50/0

the required polymerization reaction. It has been found that SiO_2 surfaces treated in ammonium hydroxide (NH_4OH) solution prior to room-temperature bonding can yield a stronger bond at low temperatures than those treated in standard RCA solution.[12,44] The SiO_2 surfaces are terminated mainly by NH_2 and OH groups after the treatment:

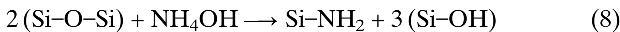

$$2\,(\text{Si–O–Si}) + NH_4OH \longrightarrow \text{Si–}NH_2 + 3\,(\text{Si–OH}) \quad (8)$$

During room-temperature bonding, it is likely that a cluster of two or three NH_3 or HOH molecules forms a bridge between the NH_2 or OH groups on the two mating surfaces. Low-temperature annealing removes NH_3 and HOH molecules and the following three reactions take place:

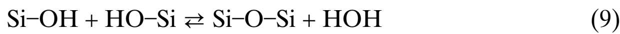

$$\text{Si–OH} + \text{HO–Si} \rightleftarrows \text{Si–O–Si} + \text{HOH} \quad (9)$$

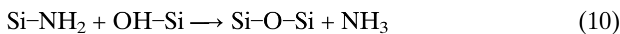

$$\text{Si–}NH_2 + \text{OH–Si} \longrightarrow \text{Si–O–Si} + NH_3 \quad (10)$$

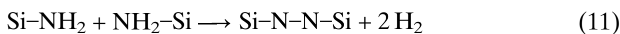

$$\text{Si–}NH_2 + NH_2\text{–Si} \longrightarrow \text{Si–N–N–Si} + 2\,H_2 \quad (11)$$

The bond energy of Si–N is 4.6 eV and is close to the 4.5 eV of the Si–O bond. The siloxane bond formation rate in polymerization reaction 9 is greatly accelerated in basic solution.[45] Since the interface water is more basic than in the standard RCA-treated case due to the presence of ammonia the increased pH could accelerate the formation of strong covalent siloxane bonds across the bonding surfaces. Since the reverse reaction in Reaction 10[46] only occurs at relatively high temperatures of ~500 °C,[47] the formed siloxane bonds should not be attacked by NH_3 at lower temperatures. The hydrogen produced in Reaction 11 can diffuse away or dissolve in the surrounding oxide, and the strong Si–N bonds will remain. Overall, the three reactions result in a higher bonding energy of SiO_2/SiO_2 bonded pairs after annealing at low temperatures (e.g., 150 °C) than observed for standard RCA-treated SiO_2/SiO_2 bonded pairs, as shown in Figure 8.

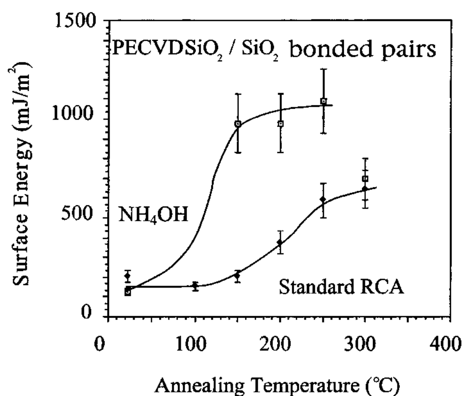

Fig. 8. Bonding energy of RCA- and NH_4OH-activated hydrophilic Si-bonded pairs as a function of annealing temperature for annealing time of 45 h at each temperature.

2.3.3. Generic Nature of Polymerization of Hydrogen-Bonded Hydrophilic Surfaces

For some metals M with relatively high electronegativity, such as those in group III or higher and some transition metals, their oxides show less ionic character and their hydroxides may also be able to polymerize at low temperatures to form a strong covalent bond:

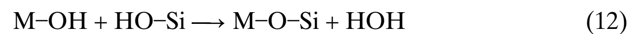

$$\text{M–OH} + \text{HO–Si} \longrightarrow \text{M–O–Si} + \text{HOH} \quad (12)$$

or

$$\text{M–OH} + \text{HO–M} \longrightarrow \text{M–O–M} + \text{HOH} \quad (13)$$

Figure 9 shows the surface energy of an oxidized Si/sapphire (Al_2O_3) bonded pair as a function of annealing time at 150 °C. It is believed that the polymerization effect is responsible for the increased bonding energy:

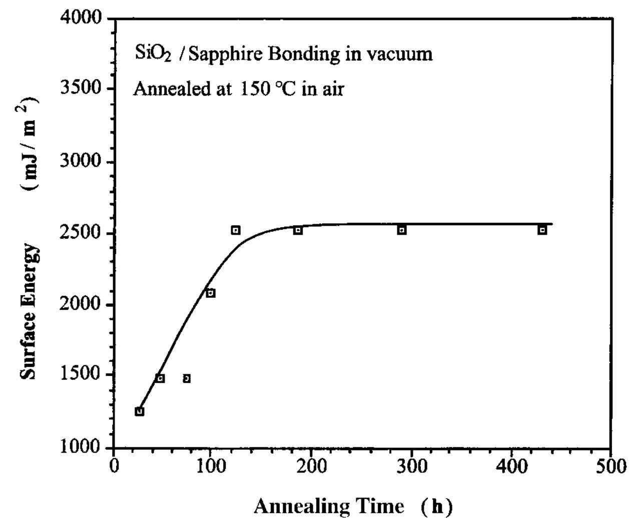

Fig. 9. Bonding energy of an oxidized Si/sapphire (Al_2O_3) bonded pair as a function of annealing time at 150 °C.

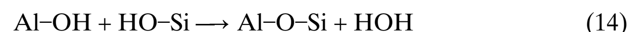

$$\text{Al–OH} + \text{HO–Si} \longrightarrow \text{Al–O–Si} + \text{HOH} \quad (14)$$

A similar reaction may also be involved in Si/ZnS bonding:[48]

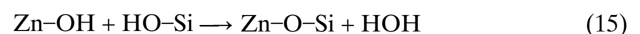

$$\text{Zn–OH} + \text{HO–Si} \longrightarrow \text{Zn–O–Si} + \text{HOH} \quad (15)$$

It was reported[35] that Si–(N_xH_y) groups can be formed on Si_3N_4 surfaces by an HF dip or NH_3 plasma treatment followed by a water rinse. Similar to Si–OH groups on Si surfaces, Si–NH groups across two bonding Si_3N_4 surfaces can also react to form strong covalent bonds at temperatures as low as 90 °C:

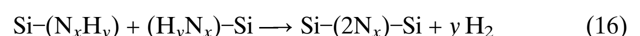

$$\text{Si–}(N_xH_y) + (H_yN_x)\text{–Si} \longrightarrow \text{Si–}(2N_x)\text{–Si} + y\,H_2 \quad (16)$$

From the above discussion, it is clear that polymerization of hydrogen-bonded hydrophilic surfaces at low tempera-

 © WILEY-VCH Verlag GmbH, D-69469 Weinheim, 1999 0935-9648/99/1712-1415 $ 17.50+.50/0

tures to form strong covalent bonds is a rather generic effect and can be applied to bonding of many different materials.

2.3.2. Low-Vacuum Bonding of Hydrophilic Wafers

Compared to bonding wafers in air, bonding of hydrophilic bare silicon wafers in low vacuum (~700 Pa or a few torr) leads to even stronger bonds at the bonding interface after annealing at temperatures as low as 150 °C.[49] The bonding energy reached is close to that of thermal silicon oxide itself. This fact would imply that the microgaps at the bonding interface caused by surface roughness of the bonding wafers are almost completely closed, possibly by the oxide formed during the low-temperature annealing. The low vacuum effects appear to be associated with a significant reduction of trapped nitrogen at the bonding interface. Trapped nitrogen prevents the intimate contact of a significant proportion of the bonding surfaces during annealing and thus prevents formation of covalent siloxane bonds. However, in order to achieve a strong bond the water generated by Reaction 7 must be removed. This argument is supported by IR spectra at the bonding interface[42] and the following experimental observations:

It was found that the oxidation reaction of Si with water at low temperatures takes place preferentially at surface steps.[50] Our experimental results have shown that low-vacuum-bonded hydrophilic Si(100) wafers with only ~0.1° miscut angle have a similar bonding energy to air-bonded pairs. On the other hand, low-vacuum-bonded hydrophilic Si(100) wafers with ~1° standard miscut angle have a much higher bonding energy than the air-bonded pairs.[44]

In recent experiments at the Max Planck Institute of Microstructure Physics (Halle, Germany) a higher bonding energy as a result of low-vacuum bonding could not be reproduced. Part of the reason for the discrepancy in results may be based on the following considerations:

According to Reaction 7, a simple estimate indicates that 1.33 cm^3 water will be required to form 1 cm^3 oxide. Assuming that the microgaps are cubes with 10 Å on each side, to fill up the gaps by oxide 44 water molecules per gap will be needed. It is known that on hydrophilic Si surfaces, each isolated OH group forms hydrogen bonds with one water molecule and each hydrogen-bonded OH group forms hydrogen bonds with two water molecules. The fully hydroxylated silica surface contains 4.6 OH groups per 100 $Å^2$. Among them 1.4 groups per 100 $Å^2$ are isolated OH groups and 3.2 groups per 100 $Å^2$ are hydrogen-bonded OH groups.[51] Therefore, if the bonding surfaces are fully saturated with OH groups ~36 water molecules (one monolayer) will be contained in the 10 Å cubes at the bonding interface. More than one monolayer of water molecules is required to oxidize the Si surrounding the microgaps. The surface coverage of molecular water on the silica surfaces depends on the relative humidity (RH): in order to have more than one monolayer on the bonding surfaces low-vacuum bonding should be performed at RH > 15 %.[27] It can also not be excluded that low-vacuum bonding mostly favors a high bonding energy in a narrow ring around the rim of the bonded wafers. Clearly, more experiments are needed to understand the effect of low vacuum on bonding energy.

There are several alternative methods to achieve strong bonding at low temperatures. An example is plasma treatment of the bonding surfaces, which cleans the surface and introduces bond defects, to enhance the chemical reactivity.

Bonding of fresh surfaces having no contamination layers should allow a covalent bond to be formed at low temperatures provided that the surfaces are reactive and not self-reconstructed into a low surface energy inert state. Experimentally, clean surfaces usually require ultrahigh vacuum (UHV) conditions. Recently, covalently bonded, large-area, and self-propagating 4 inch (100) silicon wafer pairs under UHV conditions were achieved at room temperature,[52] although not for structures containing cavities. Bonding is so strong that without any subsequent heat treatment the bonded samples fractured in tensile tests at other locations than the interface.

General speaking, a strong bond can be formed across the bonding hydrophilic surfaces of many materials during low-temperature annealing via the polymerization reaction and subsequent removal of the generated water or gas. The microgaps formed during room-temperature bonding due to the surface roughness may be fully or partially closed through i) elastic deformation resulting from an increased bonding energy and ii) oxidation of bonding materials.

2.4. Bubble-Free Bonding Interface

Even after a bubble-free (particle-free) bonding interface has been achieved during room-temperature bonding, interface bubbles can still be generated during subsequent annealing at elevated temperatures. In bonded hydrophilic bare Si wafer pairs, the hydrogen molecules resulting from Reaction 7 can not be dissolved appreciably in the silicon and therefore generate a gas pressure at the interface. In bonded hydrophobic Si wafer pairs, hydrogen molecules are also produced during annealing at temperatures higher than 300 °C:[31]

$$\text{Si–H} + \text{H–Si} \longrightarrow \text{Si–Si} + H_2 \qquad (17)$$

For good bonding, in addition to removing all particles from the bonding surfaces, one of the following methods should be adopted to prevent interface bubble generation during annealing: i) removal of hydrocarbons, which are essential in the nucleation of interface bubbles, from the bonding interface by annealing wafers at 600 °C[53] in oxygen or by careful and adequate cleaning such as in the strong oxidizer HIO_4;[54] ii) providing a hydrogen absorption bonding layer such as silicon oxide at the bonding in-

 © WILEY-VCH Verlag GmbH, D-69469 Weinheim, 1999

terface unless one of the bonding wafers itself can dissolve hydrogen molecules;[55] iii) providing a groove mesh in one of the bonding wafers to allow the hydrogen or other gases to diffuse out—grooves ~2–80 µm in width and 0.3–5 µm in depth, connected to the wafer edge, and separated from each other by up to 2.5 mm can be employed[56,57]—and iv) performing room-temperature bonding under UHV conditions.

3. Process Modules for Layer Splitting

Hydrogen-implantation-induced layer splitting is based on the fact that the implanted hydrogen atoms can embrittle the host materials. Figure 10 schematically shows the H-implantation-induced layer splitting process. Although

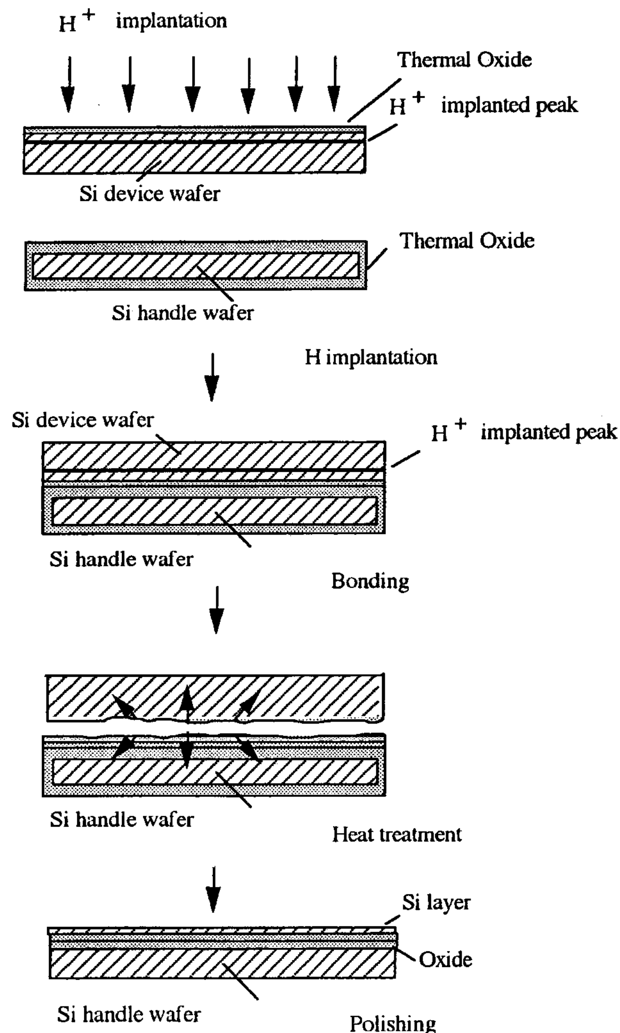

Fig. 10. Schematic of the H-implantation-induced layer splitting process.

implanted H or He can induce blisters or splitting in amorphous materials or in metals at very high doses ($>10^{18}/cm^2$), in single crystalline materials it can be achieved at medium H-implantation doses ($\sim 5 \times 10^{16}/cm^2$) due to the formation of microcracks. The formation of molecular hydrogen in the microcracks leads to an internal pressure sufficiently high to cleave the implanted layer. The basic requirements for industrially applicable layer splitting are: i) the layer can be split at reasonably low hydrogen implant doses, ii) excessive stresses and undesirable changes in the host as well as in the handling of materials can be avoided, and iii) the split layer has a smooth surface and few defects. The basic process modules to achieve these goals of layer splitting are: i) platelet formation in the host material around the peak of the implanted hydrogen concentration profile, ii) molecular hydrogen formation in the platelets, and iii) layer cleavage at low temperatures.

3.1. Platelet Formation

Although isolated H atoms can break Si–Si bonds to form Si–H bonds, it is energetically more favorable if H pairs with existing broken Si bonds. During H implantation point defects, i.e., self-interstitials and vacancies (so-called Frenkel pairs), are generated. In silicon, each implanted H ion produces approximately 10 Frenkel pairs at implant energies in the range of 30 to 100 keV. These defects provide many Si dangling bonds. The energy associated with an H atom in a Si–H pair with an existing Si dangling bond in a hydrogenated vacancy is 2.50 eV lower than when the H atom is unpaired. Similarly, the energy of H is 2.55 eV lower when the Si–H pair forms on an existing (111) or (100) surface.[58]

The formation of an H_2 molecule also leads to a reduction in energy: 0.87 eV in crystalline silicon and 1.26 eV in free space.[58] Atomic H is therefore strongly chemically reactive and there exists a driving force for H to both passivate broken Si bonds and form H_2 molecules. Impurities in Si are also defects and can be passivated by H. Atomic H reacts strongly with boron in Si resulting in 1.09 eV energy lowering. Therefore, defects in Si are strong H gettering centers.

Although H atoms diffuse quickly in defect-free monocrystalline Si even at room temperature, the actual diffusivity of H is determined by the presence of defects that trap H, reducing its mobility significantly. Similarly, the H solubility in defect-free Si is very low (only $2 \times 10^7/cm^3$ at 300 °C)[59] but its actual concentration (solubility) at low temperatures can be significantly higher when defects are available. In contrast, H_2 molecules are stable and immobile at temperatures below ~500 °C in silicon.

During the implantation process, some of the H atoms form molecular H_2 or remain as atomic H. Most of the H atoms interact immediately with the implantation-induced or pre-existing dangling bonds in silicon (X) to form a variety of X–H complexes, such as interstitial-H, multivacancy-H, and multi-H-monovacancy complexes:

$$H + X \longrightarrow X\text{–}H \quad (18)$$

 © WILEY-VCH Verlag GmbH, D-69469 Weinheim, 1999 0935-9648/99/1712-1417 $ 17.50+.50/0

If a sufficient number of vacancy-H complexes are located in close proximity, planar defects (termed "platelets") can form on (100) and (111) planes in monocrystalline Si. These platelets consist of H-passivated adjacent crystalline planes of a finite area. If the host material is severely damaged or amorphized platelet formation will not be possible. It was reported that a hydrogen dose greater than $1 \times 10^{16}/cm^2$ is required to form platelets in Si. However, only about 1/8 of the implanted hydrogen may be trapped in platelets.[60] This observation suggests that the required H dose for platelet formation will be much lower if implanted hydrogen atoms have a higher efficiency in forming platelets. It also implies that for effective layer splitting platelets should be the dominating H-trapping sites and other defects should be avoided as much as possible.

It has been observed that a low dose ($>5 \times 10^{12}/cm^2$) boron implantation preceding the H implantation with the same projected range significantly lowers the H dose required for platelet formation.[61] It is known that even at room temperature B and other group III elements in Si can be strongly passivated by H, resulting in the formation of B–H complexes:

$$B + H{-}Si \longrightarrow (B\cdots H){-}Si \tag{19}$$

Monte Carlo simulations indicate that each B atom generates ~400 Frenkel pairs. These pre-existing defects (the Frenkel pairs and B itself) greatly enhance X–H complex formation. Moreover, each B atom can trap a cluster of up to 12 H atoms[62] and the Si–H bond appears to be weakened by the presence of B next to it.[63] H atoms released from the Si–H bonds can move towards the vacancies near existing vacancy-H complexes to accelerate the formation of platelets. Therefore, the B atom appears to act as a catalyst, enhancing platelet creation during the subsequent H implantation. Experimentally, it has been shown that the enhancement effect is more significant if B is implanted prior to H implantation. A reversed order of implantation results in a much lower enhancement of platelet formation.[61] Platelet formation and layer splitting are also enhanced in heavily boron-doped silicon.[61]

It is known that if implantation is performed at elevated temperatures, some implant damage can be removed by dynamic annealing and damage accumulation can be prevented because of the enhanced mobility of point defects, which leads to an increased number of recombination or annihilation processes. In the case of H-only implantation, if H is implanted at an elevated temperature implant-induced defects would be more concentrated around the most defective region, i.e., the implanted H concentration peak, than in the case of room-temperature implantation. The lower number of competing defects for H trapping outside the implanted H peak and an increased H mobility during H implantation result in more platelets at the implanted H peak region.[16] However, the H implantation temperature must be lower than the temperature at which X–H complexes dissociate or H_2 molecules become mobile. Since an appropriate density of H-trapping defects is required for platelet formation, in order to have sufficient H-trapping defects the H implantation temperature should not be too high. On the other hand, if the H implantation temperature is too low too high a density of implant damage may result, which also prevents platelet formation.[64,65]

Recently, it has been found that in order to form an adequate density of platelets to lead to blistering on free surfaces or splitting from hydrogen-implanted monocrystalline wafers in bonded pairs, in addition to the requirement that the hydrogen dose must be above a minimum value,[66] the wafer temperature during hydrogen implantation must fall within a temperature window that is specific to each material.[67] No blistering or splitting is observed if H implantation is performed at temperatures outside its corresponding temperature window even if the H doses are much higher than the required minimum dose within the temperature windows. The approximate temperature windows for Si, SiC, GaAs, InP, c-cut sapphire, $LaAlO_3$, GaN, $LiNbO_3$, and $Pb_{0.91}La_{0.09}(Zr_{0.6}Ti_{0.4})O_3$ were determined experimentally and are listed in Table 1.

Table 1. Approximate windows of wafer temperature during H implantation required to induce blistering/splitting of Si, SiC, GaAs, InP, c-cut sapphire, $LaAlO_3$, GaN, $LiNbO_3$, and $Pb_{0.91}La_{0.09}(Zr_{0.6}Ti_{0.4})O_3$.

Monocrystalline material	Wafer temperature window
Si	~ 50–450°C
SiC	~ 50–900°C
GaAs	~ 160–250°C
InP	~ 150–250°C
GaN	~ 275–450°C
$LiNbO_3$	~ 23–500°C
$Pb_{0.91}La_{0.09}(Zr_{0.6}Ti_{0.4})O_3$	~ 23–150°C
c-cut sapphire	~ 700–850°C
$LaAlO_3$	~ 350–450°C

Generally speaking, H-induced platelets can be formed in almost any monocrystalline material provided that i) H is implanted with a sufficiently high dose, ii) amorphization of the host material is prevented in the implanted region, and iii) an adequate number of H-trapping defects are concentrated around the implanted H peak. The formation of platelets can be significantly enhanced if an adequate density of H-trapping centers pre-exists and/or H implantation is performed at appropriate elevated temperatures.

3.2. H_2 Molecule Formation in Microcracks

As discussed above, there is a driving force for the implanted H in Si to form hydrogen molecules (H_2) in free space. The platelet is a planar defect of finite area consisting of two H-passivated adjacent crystalline planes. Since the platelets are likely to be the result of the agglomeration of vacancy-H complexes, they provide the "in-diffused" H

 © WILEY-VCH Verlag GmbH, D-69469 Weinheim, 1999 0935-9648/99/1712-1418 $ 17.50+.50/0

a free space in Si to form H_2 molecules. During annealing at elevated temperatures, X–H complex dissociation occurs with the less stable X–H complexes dissociating at lower temperatures. The released H atoms diffuse into the platelets to form molecular H_2 gas, which results in the formation of microcracks and an increased internal pressure in the microcracks. The subsequent growth of the microcracks during annealing that causes blistering and splitting is a combined effect of the increased internal pressure and chemical reaction between the "in-diffused" H atoms and the strained Si–Si bonds around the rim of the microcracks.[68] The chemical reaction, given by

$$\text{Si–Si} + 2\,\text{H} \longrightarrow \text{Si–H} + \text{H–Si} \quad (20)$$

combined with the mechanical pressure in the microcracks may lead to the injection of Si interstitials, Si_I, into the host substrate when the elastic energy exceeds the Frenkel pair formation energy. The vacancy generated may be hydrogenated:

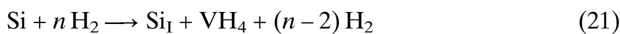

$$\text{Si} + n\,\text{H}_2 \longrightarrow \text{Si}_\text{I} + \text{VH}_4 + (n-2)\,\text{H}_2 \quad (21)$$

where n is the number of H_2 molecules in the microcracks. The reduced number of H_2 molecules provides a space for "in-diffusing" H to form H_2 molecules in the microcracks:

$$\text{H} + \text{H} \longrightarrow \text{H}_2 \quad (22)$$

It has been found that Si–Si bond breaking around the rim of the cracks is usually the rate-limiting step in the growth of microcracks because the activation energy derived from the Arrhenius relation of the blistering time as a function of annealing temperature of H-implanted Si approximately equals the Si–Si bond energy. The above relation is also approximately valid for Ge, SiC, diamond, and sapphire (Al_2O_3).[69] Figure 11 shows the experimentally determined activation energies E_a of H-implanted Si, Ge, SiC, diamond, and sapphire samples and their corresponding bond energies E_b.

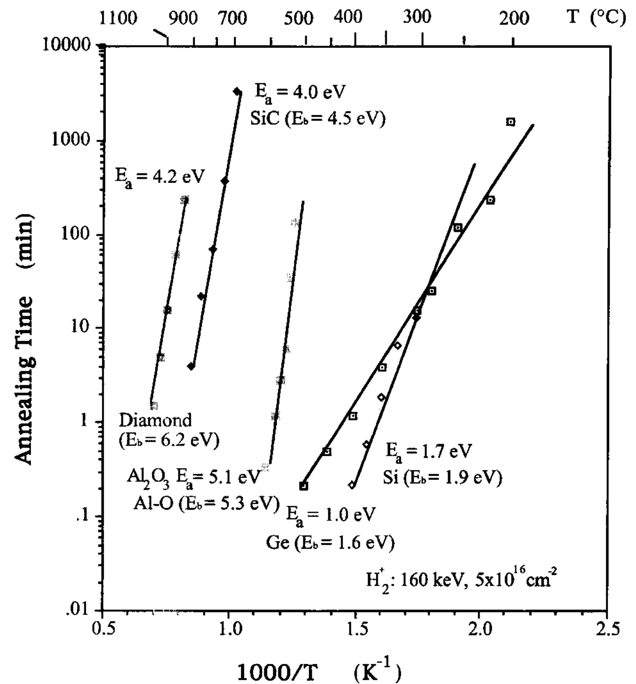

Fig. 11. Experimentally determined activation energies E_a of H-implanted Si, Ge, SiC, diamond, and sapphire samples and their corresponding bond energies E_b.

3.3. Layer Splitting at Low Temperatures

3.3.1. Surface Blistering of H-Implanted Host Materials

If the hydrogen implantation dose is above a minimum dose, surface blistering of the implanted wafer will develop during subsequent annealing because of the increased internal pressure and chemical reaction between "in-diffused" H and the Si–Si bonds at the rim of the microcracks. When the dose of implanted H is sufficiently high, e.g., $>1 \times 10^{17}/\text{cm}^2$ in Si, blisters are observed to form even without subsequent annealing. It has been found that initially the microcracks that are located around the maximum H concentration below the surface of the implanted material grow laterally until surface blisters suddenly develop after a specific annealing time (termed "blistering time") during which the microcracks reach a critical size.[70] In Si, the size of the initial platelets is usually about 50 to 250 Å in length. The critical size of the microcracks is typically in the range 1–2 µm and depends on the surface layer thickness, H implantation dose, and Young's modulus of the surface layer. This phenomenon may be understood qualitatively based on the equilibrium between the internal force of the bent layer of the blisters and the bonding force in the H-implanted rim of the blisters.

This effect allows the H-implanted wafers to be annealed prior to bonding up to the point just before surface blistering occurs. Then the pre-annealed wafer can still be bonded to a desired substrate, and the layer splitting of the implanted layer will takes place with a much lower thermal budget (lower temperatures and/or shorter times) than required without pre-annealing.[61]

In order to achieve whole layer splitting of the H-implanted wafers, surface blistering must be prevented. This can be achieved by bonding the H-implanted wafers to a desired substrate of a thickness exceeding the critical thickness, e.g., >20 µm, followed by annealing to reach a bonding energy higher than that of the H-implanted region with a thermal budget (temperature and time) lower than that required to generate blisters on the H-implanted wafer surface if the wafer were not bonded. Since the H-implanted region is greatly weakened by the generation of microcracks the average bonding energy in the H-implanted region in Si can be as low as 500 mJ/m^2, which is about 1/5 of the bonding energy of typical bulk Si.[71]

 © WILEY-VCH Verlag GmbH, D-69469 Weinheim, 1999 0935-9648/99/1712-1419 $ 17.50+.50/0

3.3.2. Low-Dose, Low-Temperature, and Low-Roughness Layer Splitting

For bonded pairs of an H-implanted wafer and a substrate, sudden layer splitting at the whole wafer scale will take place when the microcracks in the H-implanted region overlap. According to recent reports,[66,72] the minimum H dose ϕ_m for layer splitting can be estimated by

$$\phi_m = \frac{\gamma}{\alpha k T} \quad (23)$$

where γ is the bonding energy of H-implanted planes to be split during subsequent annealing, α a parameter related to the efficiency of the implanted H atoms at splitting (percentage of H atoms involved in splitting), k Boltzmann's constant, and T the absolute temperature.

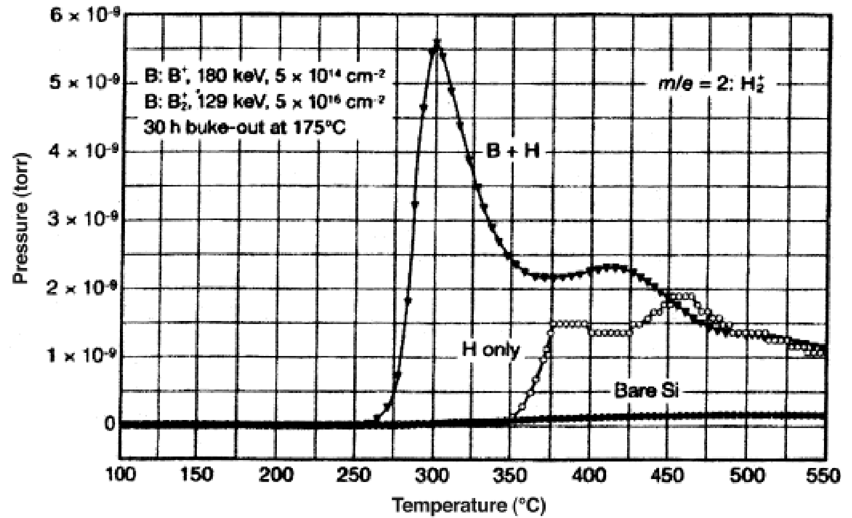

Fig. 12. H evolution with temperature for H-only and B + H co-implanted Si samples measured by quadrupole mass spectrometry.

In H-only implanted Si, it was found that only ~1/8 of the initial implanted H is involved in platelet formation and 30 % of the initially implanted H contributed to the actual layer splitting.[42] It is clear that in order to lower the minimum H dose, α should be increased.

As discussed above, to lower the minimum H dose and the thermal budget for layer splitting, one of the following four approaches can be adopted:

- B implantation with small doses ($>5 \times 10^{12}$/cm^2) prior to an implantation-peak-aligned H implantation (B + H co-implant);
- H implantation at elevated temperatures;
- Combination of the above two options, i.e., B + H co-implantation in which H is implanted at elevated temperatures;
- H implantation followed by He implantation.

To determine the minimum H dose for Si layer splitting, following a fixed B implantation at 180 keV and a dose of 5×10^{14}/cm^2, H^+ was implanted at a fixed energy of 65 keV at various doses from 1.2×10^{16}/cm^2 to 1×10^{17}/cm^2 into Si samples. In H-only implanted Si, there is no blistering observed with H doses less than 3.6×10^{16}/cm^2. However, on B + H co-implanted Si samples, blistering takes place with an H dose as low as 1.2×10^{16}/cm^2. Although splitting was not achieved at this low H dose, a whole 4 inch Si layer was transferred onto an oxidized Si wafer (SOI) with an H dose of 2.8×10^{16}/cm^2 during annealing at 400 °C. Figure 12 shows H evolution with temperature for H-only and B + H co-implanted Si samples, measured by quadrupole mass spectrometry. It is apparent that more H was incorporated in blistering in the B + H case than in the H-only implanted case, meaning a larger α is obtained. By combined B pre-implantation at 180 keV at a dose of 5×10^{14} B ions/cm^2 with a high-temperature (300 °C) implant of H at a dose of 2.0×10^{16} H ions/cm^2, a whole 4 inch Si layer was transferred onto an oxidized Si wafer (SOI) during annealing at 400 °C.[16]

Recently, it was reported that H implantation followed by He implantation enables layer splitting at a much lower total dose than required for either H or He alone.[73] It was demonstrated that the minimum dose for silicon layer splitting was achieved by H implantation at a dose of 7.5×10^{15}/cm^2 at 30 keV followed by He implantation at a dose of 1×10^{16}/cm^2 at 33 keV. In this process, H chemically interacts with the broken silicon bonds it creates during implantation to form a high density of platelets. Because He is an inert species and is not readily trapped by broken silicon bonds, it can more easily diffuse into the platelets or microcracks, resulting in crack growth that leads to splitting.

The surface mean roughness of the split Si layer is in the range of 100 Å in terms of rms (root mean square) values. There are two main causes of the surface microroughness. First, H-induced platelets/microcracks are located on (100) and (111) planes in Si independent of the surface orientation of the wafers being implanted. A close inspection of transmission electron microscopy (TEM) images of microcracks in H-implanted Si indicates that after annealing the dominating crack consists of connecting (100) and (111) microcracks. For a (100) wafer, the surface microroughness is determined by the length of the (111) microcracks that connect the two (100) internal surfaces.[42] Therefore, any technique that can increase the density of (100) and (111) microcracks will result in smoothing the split surfaces. Obviously, B implantation increases the density of the (111) and (100) microcracks significantly, leading to a reduced surface roughness.[16]

Another factor that effects the surface roughness of the split layer is the bonding energy of the bonded pair of an H-implanted wafer and a substrate. In the extreme case of a very weak bond, surface blistering instead of layer splitting will occur in the H-implanted wafer of the bonded

 © WILEY-VCH Verlag GmbH, D-69469 Weinheim, 1999 0935-9648/99/1712-1420 $ 17.50+.50/0

pairs. The surface of the blistering wafer shows a topography on the order of 1–2 μm even though the density of (100) and (111) microcracks can be very high. It has been demonstrated that at a bonding energy of >1000 mJ/m^2 before the splitting temperature a surface roughness of ~10 Å is achieved.[16] At present, the mechanism involved in this process is not clear.

Based on the above discussion, layer transfer by wafer bonding and B + H or H-only implanted layer splitting should work for almost all solids provided that: i) H can passivate B and the broken bonds (X) of the host material and form H-stabilized platelets. ii) It is energetically favorable that H_2 molecules form in the gap of the platelets. iii) H_2 molecules are immobile and stable below a reasonable critical temperature. A sufficient amount of H_2 molecules must be accumulated in the microcracks by diffusion of the H atoms released from the B–H and X–H complexes during annealing at temperatures lower than the critical temperature. iv) The amount of damage that occurs before or during implantation should be within an adequate range. As discussed above, too high or too low an implantation damage level will prevent splitting taking place. v) The bonding energy of bonded pairs must be higher than the bonding energy of the H-implanted region in the host material at the splitting temperatures.

4. Application Examples

4.1. InP Layer Transfer onto Si Wafer

Transfer of a thin layer of a compound semiconductor onto a Si substrate leads to a new materials system in which integration of compound semiconductor optoelectronic devices with silicon signal processing circuits can be realized. On top of the thin layer, other compound semiconductors or quaternaries can be grown epitaxially. The materials system has a thermal conductivity and a mechanical strength very close to that of silicon, which is usually much better than that of compound semiconductors. The wafer size and thickness of the materials system can therefore match that of silicon and the well-developed silicon technology can be employed.

Recently, InP layer transfer onto Si wafer was demonstrated using wafer bonding and H-implanted layer splitting.[12] The InP wafers employed were 3 inches in diameter, had (100) orientation, were Fe doped, had $>1 \times 10^7$ Ω cm of resistivity, and were 600 μm thick. The Si wafers used were 3 inches in diameter, had (100) orientation, were B doped, had 8–10 Ω cm of resistivity, and were 400 μm thick. In order to form an adequate density of platelets, as discussed above, the temperature of the InP wafers during H implantation has to be between ~150 and ~250 °C in the H-only implantation case. No blistering or splitting is observed during subsequent annealing if the wafer temperature during hydrogen implantation is outside the specific temperature window even though the H dose is $2 \times 10^{17}/cm^2$, which is much higher than the minimum dose required for layer splitting within the appropriate temperature window. The required H implantation temperatures are somewhat lower in the case of B + H co-implantation than in the H-only implantation case. It appears that similar to the situation in Si, boron atoms in InP serve as catalysts and can form B–H complexes, which dissociate at low temperatures, and the mobility of the released hydrogen atoms is enhanced at elevated temperatures during hydrogen implantation. All these factors assist platelet/microcrack formation.

It has been found that using ammonium hydroxide instead of standard RCA solution for SiO_2 surface activation, the bonding energy of bonded PECVD SiO_2 to SiO_2 pairs can reach up to ~1000 mJ/m^2 at an annealing temperature of 150 °C, which is sufficiently high for layer splitting. In Figure 8 a comparison of bonding energy as a function of annealing temperature of PECVD SiO_2/SiO_2 pairs using RCA or ammonium hydroxide treatment prior to room-temperature bonding is made.

The InP wafers were coated with a 3500 Å thick PECVD SiO_2 layer at 250 °C and annealed at 300 °C for 50 h to drive off trapped hydrogen in the oxide layer. The InP wafers were then implanted with B^+ at 190 keV and a dose of 5×10^{14} cm^{-2} at room temperature followed by hydrogen implantation at 108 keV and a dose of 3.5×10^{16} H_2^+ cm^{-2} at 90 °C. The peaks of the two implantation profiles were aligned. In order to achieve a bondable surface, CMP (chemical mechanical polishing) of the oxide-coated InP wafers was performed for 10 min. The 3 inch InP wafers were then cleaned in a standard RCA1 solution, followed by activation in ammonium hydroxide prior to bonding to a 2500 Å thick thermal oxide–coated 3 inch Si wafer in low vacuum. The bonded InP/Si pairs were annealed at 100 °C for 50 h to increase the bonding energy. This was followed by 150 °C annealing to split the InP layers and transfer them onto the Si substrates.

4.2. Layer Transfer for Insulator on Semiconductor (IOS)

Similar to the conventional SOI (silicon-on-insulator or semiconductor-on-insulator) materials, reversed SOI, i.e., IOS (insulator-on-semiconductor) is also a very useful kind of material combination. For high-frequency mobile communication systems, a thin layer of piezoelectric or ferroelectric oxide crystals such as quartz, $LiTaO_3$, or $LiNbO_3$ on Si is required for high Q-factor and low temperature coefficient miniaturized surface acoustic wave filters, surface and bulk resonators, and oscillators. Combining these materials with Si can lead to the integration of electronic and acoustic devices (so-called integrated electroacoustic devices) on the same chip. Voltage-controlled and temperature-compensated high Q-factor crystal oscillators, crystal resonators with Si oscillators, and filters on a chip can also

 © WILEY-VCH Verlag GmbH, D-69469 Weinheim, 1999 0935-9648/99/1712-1421 $ 17.50+.50/0

be realized. The integration of high-performance GaAs photodetectors with $LiNbO_3$ waveguides makes integrated optical circuits possible. By preparing a thin layer of single crystalline transition metal oxides such as magnetic garnets on Si or III–V semiconductors, stabilized laser diodes can be realized due to the availability of on-chip thin-film optical isolators and circulators. However, the results reported to date were all done on small samples (<10 mm × 10 mm) and involved relatively thick layers (~15–20 μm) because of the large thermal mismatch and non-uniformity of mechanical lapping. Layer transfer by wafer bonding and layer splitting provides a unique opportunity to prepare IOS material combinations efficiently.

4.2.1. Sapphire Layer Transfer onto Si

A thin layer of sapphire (Al_2O_3) on Si wafer is desirable for MEMS (microelectromechanical system) devices, such as high temperature pressure sensors and etch-stop layers. Although single-crystal Al_2O_3 films with (100) orientation can be epitaxially grown on Si(100),[74] a c-cut sapphire film of [0001] orientation can only be transferred onto Si from a bulk c-cut sapphire wafer. The c-cut sapphire layer on Si could be used to integrate Si with GaN on the same chip, in which a GaN film is epitaxially grown on the sapphire on Si for integration of blue-light lasers and Si signal processing devices. Recently, it has been demonstrated that surface blistering and layer splitting of sapphire is possible if H implantation is performed at elevated temperatures within a temperature window of approximately 700–850 °C for the sapphire wafer. In our experiments the temperature of the wafer holder during implantation was about 100 °C lower than the actual wafer temperature.

The c-cut sapphire wafers used were 2 inches in diameter and were implanted by H_2^+ at 160 keV at a dose of $5 \times 10^{16}/cm^2$ in the above-given temperature window. Surface blisters developed during the subsequent annealing from 500 to 1000 °C. The blistering time as a function of annealing temperature of the H-implanted sapphire is shown in Figure 11. It shows an Arrhenius relation very similar to that in H-implanted Si. The activation energy of ~5.1 eV is also close to the bond energy (5.3 eV) of Al–O bonds. These results suggest that the blistering process in H-implanted single crystalline c-cut sapphire is similar to that in H-implanted Si. TEM images of as-implanted c-cut sapphire that was implanted by H_2^+ at a dose of $5 \times 10^{16}/cm^2$ at an energy of 160 keV at 450 °C and 750 °C, are shown in Figure 13a and b, respectively. The $[01\bar{1}0]$ platelets and microcracks are clearly shown in both samples. The size of these defects is more than 100 % larger in the 750 °C sample than in the 450 °C implanted samples. A large crack along with many bubbles in the middle of the defective region is observed in the 750 °C case. Based on the Monte Carlo simulator Trim95, the number of defects created by H implantation in sapphire is about a factor of three larger than in Si for the same implantation dose and energy. This fact suggests that the H-implantation temperature is necessarily higher for sapphire than for Si in order to form microcracks. However, H-implantation temperatures higher than 900 °C were found to be too high to form blisters, probably due to "out-diffusion" of H_2 molecules.

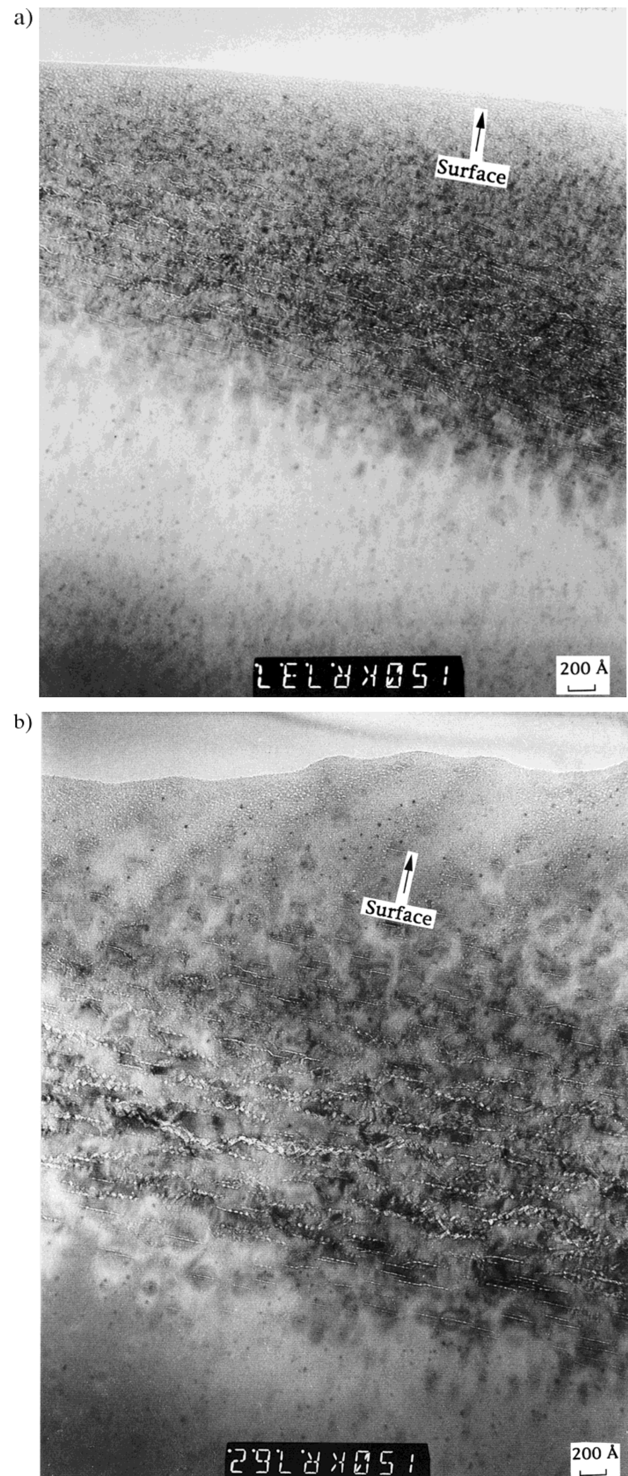

Fig. 13. TEM images of platelets in as-implanted c-cut sapphire that was implanted by H_2^+ at a dose of $5 \times 10^{16}/cm^2$, an energy of 160 keV, and a temperature of a) 450 °C and b) 750 °C.

© WILEY-VCH Verlag GmbH, D-69469 Weinheim, 1999
0935-9648/99/1712-1422 $ 17.50+.50/0

ADVANCED MATERIALS

The H-implanted 2 inch diameter c-cut sapphire wafers (H_2^+ dose of 5×10^{16}/cm^2, energy of 160 keV) were bonded to Si(100) wafers and annealed at 250 °C to strengthen the bond. After cutting the bonded pairs into smaller pieces to reduce the risk of breakage due to thermal stress, the samples were annealed between 625 and 800 °C. Thin sapphire stripes 0.4 µm thick and 10 mm × 2 mm in size were transferred from the sapphire onto the Si.

4.2.2. $LaAlO_3$ Layer Transfer

Blistering and layer splitting were also observed in H-implanted $LaAlO_3$.[15] It was found that in order for $LaAlO_3$(100) to achieve blistering and layer splitting with an H_2^+ dose of 3.5–5.0 × 10^{16}/cm^2 H implantation must be performed on a wafer in the temperature range ~450 to ~550 °C. For the $LaAlO_3$ samples that were implanted by H_2^+ at 450 °C at an H_2 dose of 5×10^{16}/cm^2 at 160 keV the blistering time as a function of annealing temperature is given in Figure 14. Again, an Arrhenius relation is observed and the activation energy is about 1.7 eV.

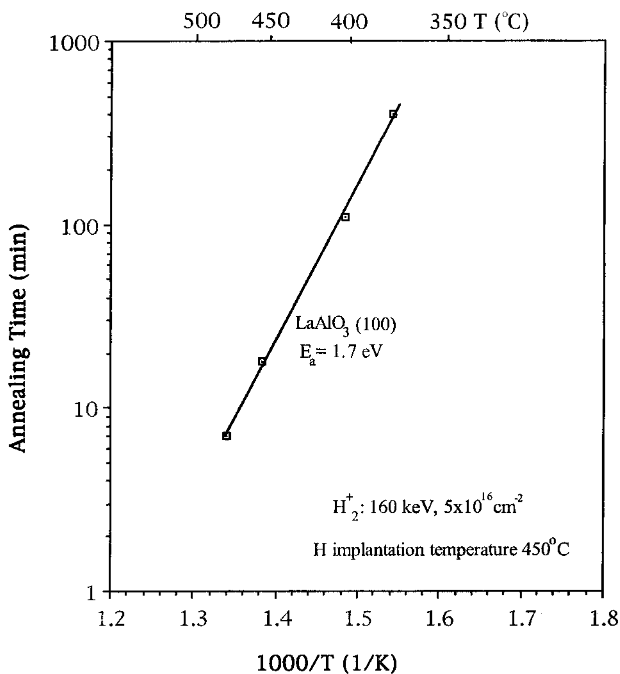

Fig. 14. Blistering time as a function of annealing temperature of $LaAlO_3$ samples that were implanted by H_2^+ at 450 °C with an H_2 dose of 5×10^{16}/cm^2 at 160 keV.

5. Conclusions

In this review two of the fundamental technologies for microsystem fabrication, i.e., wafer bonding and layer splitting were discussed in terms of their basic process modules. Both wafer bonding and layer splitting are generic in nature and may be used for many materials.

Direct bonding of almost any solid material appears to be possible via van der Waals forces of attraction provided the bonding surfaces are sufficiently smooth, flat, and clean. OH-, NH-, or FH-terminated hydrophilic bonding surfaces allow a strong bond to be developed during annealing at low temperatures via polymerization reactions and removal of the by-products.

Layer splitting of any crystalline material appears feasible with H-only or B + H co-implantation at a reasonable dose, with the materials being implanted at temperatures in a window that is specific to each material. These conditions allow adequate defects for platelets to be created and for stable H_2 molecules to be formed in the platelets, which leads to an increased internal pressure in the microcracks formed, which in turn causes layer splitting.

As shown in Figure 15, layer transfer can also be achieved by wafer bonding and layer peeling realized by a mechanical force such as a pressurized gas layer (a gas blade).[75] Since the H-implanted region is embrittled a mechanical force can peel off the H-implanted layer from its

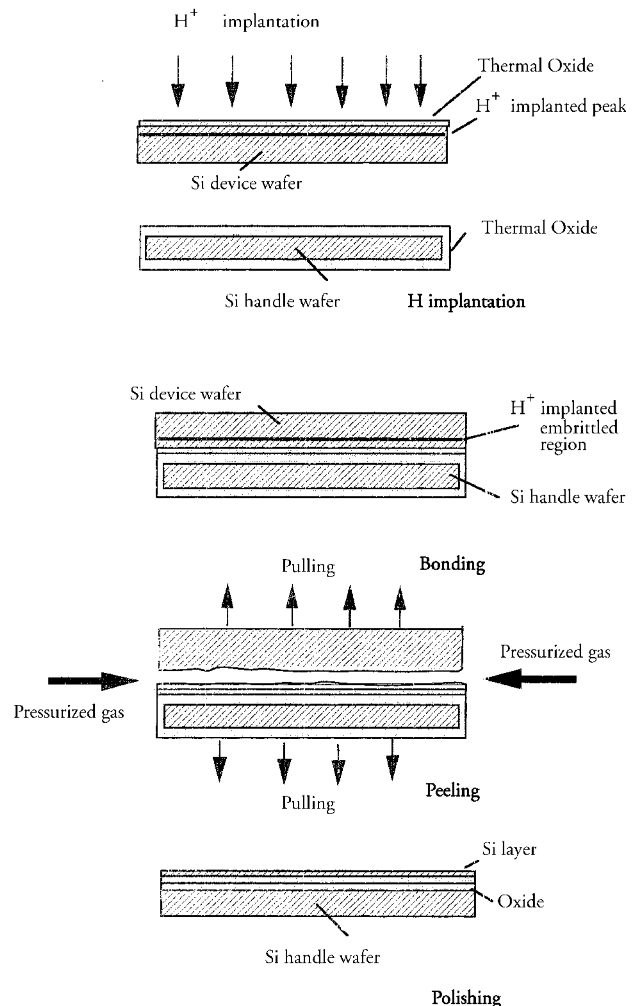

Fig. 15. Schematic of the H-induced embrittlement and layer peeling process.

 © WILEY-VCH Verlag GmbH, D-69469 Weinheim, 1999 0935-9648/99/1712-1423 $ 17.50+.50/0

host substrate if the bonding energy at the bonding interface is much higher than that in the H-implanted region. Thus, layer transfer at room temperature can be realized.

Overall, wafer bonding and layer splitting combined represent a versatile and practical materials as well as device technology. Applications appear to be more limited by our lack of imagination than by practical constraints.

Received: June 1, 1999

[1] L. Rayleigh, *Proc. Phys. Soc.* **1936**, *A156*, 326.
[2] M. Shimbo, K. Furukawa, K. Fukuda, K. Tanzawa, *J. Appl. Phys.* **1986**, *60*, 2987.
[3] J. B. Lasky, *Appl. Phys. Lett.* **1986**, *48*, 78.
[4] P. W. Barth, *Sens. Actuators A* **1990**, *21–23*, 91.
[5] J. Haisma, B. A. C. M. Spierings, U. K. P. Biermann, A. A. van Gorkum, *Appl. Opt.* **1994**, *33*, 1154.
[6] Q.-Y. Tong, U. Gösele, *Mater. Chem. Phys.* **1994**, *37*, 101.
[7] G. Cha, R. Gafiteanu, Q.-Y. Tong, U. Gösele, in *2nd Int. Symp. on Semiconductor Wafer Bonding: Science, Technology, and Applications* (Eds: H. Baumgart, C. Hunt, M. Schmidt, T. Abe), Electrochem. Soc. Proc. Vol. 93-29, Electrochemical Society, Pennington, NJ **1993**, p. 257.
[8] M. Bruel, *Electron. Lett.* **1995**, *31*, 1201.
[9] T.-H. Lee, Q.-Y. Tong, Y.-L. Chao, L.-J. Huang, U. Gösele, *Proc. IEEE Int. SOI Conf.* **1997**, *97CH36 069*, 40.
[10] L. Di Cioccio, Y. Le Tiec, F. Letertre, C. Jaussaud, M. Bruel, *Electron. Lett.* **1996**, *32*, 1144.
[11] Q.-Y. Tong, T.-H. Lee, P. Werner, U. Gösele, R. B. Bergmann, J. H. Werner, *J. Electrochem. Soc.* **1997**, *144*, L111.
[12] Q.-Y. Tong, Y.-L. Chao, L.-J. Huang, U. Gösele, *Electron. Lett.* **1999**, *35*, 341.
[13] E. Jalaguier, B. Aspar, S. Pocas, J. F. Michaud, M. Zussy, A. M. Papon, M. Bruel, *Electron. Lett.* **1998**, *34*, 408.
[14] T. Tanaka, H. Horie, S. Ando, S. Hijiya, *Tech. Dig.—Int. Electron Devices Meet.* **1991**, 683.
[15] L.-J. Huang, Q.-Y. Tong, Y.-L. Chao, U. Gösele, *Electrochem. Solid State Lett.* **1999**, *May*, 238.
[16] Q.-Y. Tong, R. Bower, *MRS Bull.* **1998**, *23*, 40.
[17] *1st Int. Symp. on Semiconductor Wafer Bonding: Science, Technology, and Applications* (Eds: U. Gösele, J. Haisma, M. Schmidt, T. Abe), Electrochem. Soc. Proc. Vol. 92-7, Electrochemical Society, Pennington, NJ **1992**.
[18] *2nd Int. Symp. on Semiconductor Wafer Bonding: Science, Technology, and Applications* (Eds: H. Baumgart, C. Hunt, M. Schmidt, T. Abe), Electrochem. Soc. Proc. Vol. 93-29, Electrochemical Society, Pennington, NJ **1993**.
[19] *3rd Int. Symp. on Semiconductor Wafer Bonding: Science, Technology, and Applications* (Eds: H. Baumgart, C. Hunt, S. Iyer, U. Gösele, T. Abe), Electrochem. Soc. Proc. Vol. 95-7, Electrochemical Society, Pennington, NJ **1995**.
[20] *4th Int. Symp. on Semiconductor Wafer Bonding: Science, Technology, and Applications* (Eds: U. Gösele, H. Baumgart, C. Hunt, T. Abe), Electrochem. Soc. Proc. Vol. 97-36, Electrochemical Society, Pennington, NJ **1998**.
[21] W. P. Maszara, *J. Electrochem. Soc.* **1991**, *138*, 341.
[22] S. Bengtsson, *J. Electron. Mater.* **1992**, *21*, 841.
[23] A. Plößl, G. Krauter, *Mater. Sci. Eng. Rev.*, **1999**, *25*, 1.
[24] M. Bruel, *MRS Bull.* **1998**, *23*, 35.
[25] U. Gösele, Q.-Y. Tong, *Annu. Rev. Mater. Sci.* **1998**, *28*, 215.
[26] Special Issue on Direct Bonding, *Philips J. Res.* **1995**, *49*, 1.
[27] Q.-Y. Tong, U. Gösele, *Semiconductor Wafer Bonding: Science and Technology*, Wiley, New York **1998**.
[28] C. Kittel, *Introduction to Solid State Physics*, Wiley, New York **1986**.
[29] J. Del Bene, J. A. Pople, *J. Chem. Phys.* **1970**, *52*, 4858.
[30] Q.-Y. Tong, T.-H. Lee, U. Gösele, M. Reiche, J. Ramm, E. Beck, *J. Electrochem. Soc.* **1997**, *144*, 384.
[31] Q.-Y. Tong, E. Schmidt, U. Gösele, M. Reiche, *Appl. Phys. Lett.* **1994**, *64*, 625.
[32] H. Nakanishi, T. Nishimoto, R. Nakamura, A. Yotsumoto, S. Shoji, in *Proc. MEMS Systems 98*, IEEE, Piscataway, NJ **1998**, *CH36 176*, p. 609.
[33] T. A. Michalske, E. R. Fuller, *J. Am. Ceram. Soc.* **1985**, *68*, 586.
[34] T. Abe, J. H. Matlock, *Solid State Technol.* **1990**, *November*, 39.
[35] R. W. Bower, M. S. Ismail, B. E. Roberds, *Appl. Phys. Lett.* **1993**, *28*, 2485.
[36] W. P. Maszara, G. Goetz, A. Caviglia, J. B. McKitterick, *J. Appl. Phys.* **1988**, *64*, 4943.
[37] W. P. Maszara, B.-L. Jiang, A. Yamada, G. A. Rozgoni, H. Baumgart, A. J. R. De Kock, *J. Appl. Phys.* **1991**, *69*, 257.
[38] S. Mack, H. Baumann, U. Gösele, H. Werner, R. Schlögl, *J. Electrochem. Soc.* **1997**, *144*, 1106.
[39] Q.-Y. Tong, U. Gösele, *J. Electrochem. Soc.* **1995**, *142*, 3975.
[40] R. Stengl, K.-Y. Ahn, U. Gösele, *Jpn. J. Appl. Phys.* **1989**, *27*, L2364.
[41] Q.-Y. Tong, G. Cha, R. Gafiteanu, U. Gösele, *IEEE J. Microelectromech. Syst.* **1994**, *3*, 29.
[42] M. K. Weldon, V. E. Marsico, Y. J. Chabal, A. Agarwal, D. J. Eaglesham, J. Sapjeta, W. L. Brown, D. C. Jacobson, Y. Caudano, S. B. Christman, E. E. Chaban, in *4th Int. Symp. on Semiconductor Wafer Bonding: Science, Technology, and Applications* (Eds: U. Gösele, H. Baumgart, C. Hunt, T. Abe), Electrochem. Soc. Proc. Vol. 97-36, Electrochemical Society, Pennington, NJ **1998**, p. 229.
[43] J. Jiao, D. Lu, B. Xiong, W. Wang, *Sens. Actuators A* **1995**, *50*, 117.
[44] Y.-L. Chao, *Master's Thesis*, Duke University **1998**.
[45] R. K. Iler, *The Chemistry of Silica*, Wiley, New York **1979**, p. 373.
[46] Y. Z. Hu, R. J. Gutmann, T. P. Chow, *J. Electrochem. Soc.* **1998**, *145*, 3919.
[47] E. F. Vansant, P. van der Voort, K. C. Vrancken, *Characterization and Chemical Modification of the Silica Surface*, Elsevier, Amsterdam **1995**, p. 387.
[48] T. Feng, Q.-Y. Tong, J. Askinazi, U. Gösele, in *3rd Int. Symp. on Semiconductor Wafer Bonding: Science, Technology, and Applications* (Eds: H. Baumgart, C. Hunt, S. Iyer, U. Gösele, T. Abe), Electrochem. Soc. Proc. Vol. 95-7, Electrochemical Society, Pennington, NJ **1995**, p. 597.
[49] Q.-Y. Tong, W. J. Kim, T.-H. Lee, U. Gösele, *Electrochem. Solid State Lett.* **1998**, *1*, 52.
[50] T. Sunada, T. Yasaka, M. Takakura, T. Sigiyama, S. Miyazaki, M. Hirose, *Jpn. J. Appl. Phys.* **1990**, *29*, L2408.
[51] C. G. Armistead, A. J. Tyler, F. H. Hambleton, S. A. Mitchell, J. A. Hockey, *J. Phys. Chem.* **1969**, *73*, 3947.
[52] U. Gösele, H. Stenzel, T. Martini, J. Steinkirchner, D. Conrad, K. Scheerschmidt, *Appl. Phys. Lett.* **1995**, *67*, 3614.
[53] K. Mitani, V. Lehmann, R. Stengl, D. Feijoo, U. Gösele, H. Z. Massoud, *Jpn. J. Appl. Phys.* **1991**, *30*, 615.
[54] Q.-Y. Tong, G. Kaido, L. Tong, M. Reiche, F. Shi, J. Steinkirchner, T. Y. Tan, U. Gösele, *J. Electrochem. Soc.* **1995**, *142*, L201.
[55] T. Abe, K. Ohki, A. Uchiyama, K. Nakazawa, Y. Nakazato, *Jpn. J. Appl. Phys.* **1994**, *33*, 514.
[56] W. Kissinger, G. Kissinger, in *1st Int. Symp. on Semiconductor Wafer Bonding: Science, Technology, and Applications* (Eds: U. Gösele, J. Haisma, M. Schmidt, T. Abe), Electrochem. Soc. Proc. Vol. 92-7, Electrochemical Society, Pennington, NJ **1992**, p. 71.
[57] H. Yamaguchi, S. Fujino, T. Hattori, Y. Hamakawa, *Jpn. J. Appl. Phys.* **1995**, *34*, L199.
[58] C. G. Van der Walle, *Phys. Rev. B.* **1994**, *49*, 4579.
[59] S. J. Pearton, J. W. Corbett, T. S. Shi, *Appl. Phys. A* **1987**, *43*, 153.
[60] S. Romani, J. H. Evans, *Nucl. Instrum. Methods Phys. Res.* **1990**, *B44*, 313.
[61] Q.-Y. Tong, R. Scholtz, U. Gösele, T.-H. Lee, L.-J. Huang, Y.-L. Chao, T. Y. Tan, *Appl. Phys. Lett.* **1998**, *72*, 49.
[62] J. T. Borenstein, J. W. Corbett, S. J. Pearton, *J. Appl. Phys.* **1993**, *73*, 2751.
[63] J. I. Pankove, P. J. Zanzucchi, C. W. Magee, G. Lucovsky, *Appl. Phys. Lett.* **1985**, *46*, 421.
[64] V. C. Venzia, T. Haynes, A. Agarwal, D. Eaglesham, O. Holland, M. Weldon, Y. Chabal, in *Proc. 8th Int. Symp. Silicon Materials Science and Technology* (Eds: H. R. Huff, U. Gösele), Electrochemical Society, Pennington, NJ **1998**, Vol. 98-1, p. 1385.
[65] W. K. Chu, R. H. Kastl, R. F. Lever, S. Mader, B. J. Masters, *Phys. Rev. B* **1977**, *16*, 3851.
[66] L. B. Freund, *Appl. Phys. Lett.* **1997**, *70*, 3519.
[67] Q.-Y. Tong, L.-J. Huang, Y.-L. Chao, R. Scholtz, U. Gösele, unpublished.
[68] Q.-Y. Tong, T.-H. Lee, L.-J. Huang, Y.-L. Chao, W. J. Kim, R. Scholz, T. Y. Tan, U. Gösele, in *4th Int. Symp. on Semiconductor Wafer Bonding: Science, Technology, and Applications* (Eds: U. Gösele, H. Baumgart, C. Hunt, T. Abe), Electrochem. Soc. Proc. Vol. 97-36, Electrochemical Society, Pennington, NJ **1998**, p. 521.
[69] Q.-Y. Tong, K. Gutjahr, S. Hopfe, U. Gösele, T. H. Lee, *Appl. Phys. Lett.* **1997**, *70*, 1390.

 © WILEY-VCH Verlag GmbH, D-69469 Weinheim, 1999

[70] L.-J. Huang, Q.-Y. Tong, Y.-L. Chao, T.-H. Lee, T. Martini, U. Gösele, *Appl. Phys. Lett.* **1999**, *74*, 982.
[71] M. Bruel, B. Aspar, C. Maleville, H. Moriceay, A. J. Auberton-Herve, T. Barge, in *Proc. 8th Int. Symp. on Silicon-on-Insulator Technology and Devices* (Eds: C. Cristoloveanu, P. L. F. Hemment, K. Izumi, S. Wilson), Electrochemical Society, Pennington, NJ **1997**, Vol. 97-23, p. 3.
[72] L. J. Huang, Q.-Y. Tong, T.-H. Lee, Y.-L Chao, U. Gösele, in *8th Int. Symp. on Silicon Materials Science and Technology* (H. R. Huff, U. Gösele), Electrochemical Society, Pennington, NJ **1998**, Vol. 98-1, p. 1341.
[73] A. Agarwal, T. E. Haynes, V. C. Venezia, O. W. Holland, *Appl. Phys. Lett.* **1998**, *72*, 1086.
[74] M. Ishida, H. Kim, T. Kimura, T. Nakamura, *Sens. Actuators A* **1996**, *53*, 340.
[75] W. G. En, I. J. Malik, M. A. Bryan, S. Farrens, F. J. Henley, N. W. Cheung, C. Chan, *Proc. IEEE Int. SOI Conf.* **1998**, *P8CH36199*, 163.

———————

 © WILEY-VCH Verlag GmbH, D-69469 Weinheim, 1999 0935-9648/99/1712-1425 $ 17.50+.50/0